ISSN 0915-633X

NATIONAL INSTITUTE FOR FUSION SCIENCE

Computational Study of Three Dimensional MHD Equilibrium with m/n=1/1 Island

R. Kanno, N. Nakajima, M. Okamoto and T. Hayashi

(Received - Nov. 27, 2002)

NIFS-767 Dec. 2002

TOKI, JAPAN

Computational Study of Three Dimensional MHD Equilibrium with m/n=1/1 Island

R. Kanno†‡, N. Nakajima†‡, M. Okamoto†‡, and T. Hayashi†‡

† National Institute for Fusion Science, Toki, 509-5292, Japan

‡ Department of Fusion Science, Graduate University for Advanced Studies, Toki, 509-5292, Japan

E-mail: kanno@nifs.ac.jp

Abstract. A modification of the three dimensional MHD equilibrium code, HINT, is proposed to analyze a Large Helical Device (LHD) equilibrium with an $m/n = 1/1$ island. The equilibrium analysis is required in the local island divertor (LID) experiment, in order not only to measure structures of magnetic field lines but also to lead an optimized condition of the equilibrium. In a calculation of the equilibrium with the island, there is a numerical difficulty caused from the fact that a derivative of the pressure at the separatrix of the island is not well-behaved; i.e. it is diverged. The modified scheme has the ability to resolve the problem, and achieves the numerically appropriate analysis of an MHD equilibrium with such an island.

1. Introduction

Computational study of a three dimensional (3D) MHD equilibrium with an $m/n = 1/1$ island is reported in this article, which is carried out by using the 3D MHD equilibrium code, HINT [1, 2, 3, 4, 5, 6, 7, 8, 9], where m is a poloidal mode number and n a toroidal mode number. Especially, an equilibrium analysis of a Large Helical Device (LHD) equilibrium with an $m/n = 1/1$ island is considered. Recently, the HINT code, which does not assume the existence of nested flux surfaces, was modified so that net toroidal currents, coil currents and islands yielding Fourier components of magnetic fields with a period of full torus can exist in the computation region [7, 8, 9]. Formation or healing of magnetic islands can be investigated in a realistic LHD configuration.

An LHD equilibrium with the $m/n = 1/1$ island is required in the local island divertor (LID) experiment [10, 11]. The LID is a divertor which uses the $m/n = 1/1$ island formed at the edge region, and the island is generated by using the island control coils. The LID has been proposed to control the edge plasma of LHD. Control of the edge plasma by means of the LID is expected to realize the high temperature divertor operation which leads to a significant energy confinement improvement. Results of HINT computations are not only useful to measure flux surfaces, islands and ergodic field lines in the LID experiment but also can lead to an optimized condition in the experiment from the viewpoint of an MHD equilibrium, e.g. the optimizations of external currents

in the island control coils and profiles of rotational transform modified by net toroidal currents, etc. In previous studies of structures of the $m/n = 1/1$ island and ergodic field lines, these structures were calculated by using only vacuum field data [12, 13] or field data which are given by superimposing the peripheral field predicted by the DIAGNO code [14, 15] on the vacuum field [16]. The analysis by using only vacuum field neglects the fact that these structures are affected by the Pfirsch-Schlüter current and net toroidal currents including a bootstrap current, and one by using the DIAGNO code, which calculates the response from a finite beta equilibrium given by the free boundary equilibrium code VMEC [17], assumes the existence of nested good flux surfaces; thus they are not enough to treat the peripheral structure. The realistic analysis of the LHD equilibrium is indispensable in the LID experiment and it needs to be carried out by an appropriate numerical tool, e.g. the HINT code. However, in execution of the equilibrium analysis, we find a numerical difficulty in the standard scheme of HINT, which is caused from the fact that a derivative of the pressure at the separatrix of the island is not well-behaved, if the pressure profile in the island is almost flat, as is shown later. The difficulty is remarkable when the island yields different Fourier components of magnetic fields from ones with a toroidal period of helical coils (or external coils except island control coils); if the island has the Fourier components with the toroidal period, this problem is not so serious. In order to resolve this numerical problem, the scheme should be modified.

The organization of the following sections as follows. First of all, the standard scheme of the HINT code is introduced briefly in section 2. And in section 3 we discuss the numerical problem and propose the modified scheme. Section 4 presents the conclusions.

2. Standard scheme of HINT computation

In the HINT code, an MHD equilibrium is obtained starting from an arbitrary non-equilibrium initial plasma and vacuum field configuration by means of a time-dependent relaxation method with a small value of resistivity η. We have been developing the scheme of HINT computation over ten years, and the improvements of the scheme are scattered in several papers. We should summarize the standard version of HINT in this section.

The equilibrium calculation in HINT is carried out on the Eulerian coordinates (u^1, u^2, u^3), which may be called the helical coordinates. The relation between the helical coordinates (u^1, u^2, u^3) and the Cartesian coordinates (x, y, z) is given as

$$x = \left(R_0 + u^1_* \cos(hu^3) + u^2_* \sin(hu^3)\right) \cos(u^3), \tag{1}$$

$$y = -\left(R_0 + u^1_* \cos(hu^3) + u^2_* \sin(hu^3)\right) \sin(u^3), \tag{2}$$

$$z = -u^1_* \sin(hu^3) + u^2_* \cos(hu^3), \tag{3}$$

with

$$u^1_* = u^1 + \delta_c \cos(hu^3), \tag{4}$$

$$u^2_* = u^2 - \delta_c \sin(hu^3), \tag{5}$$

where $h = \mathrm{sgn(w)}M/2$, sgn(w) is the sign of winding of the equilibrium (i.e. sgn(w) = +1 for the left hand winding and sgn(w) = −1 for the right hand winding; e.g. sgn(w) = −1 for LHD), M the pitch number of the helical coils (e.g. $M = 10$ for LHD), $R_0 = $ const. the average major radius (e.g. $R_0 = 3.6$ m in this article), and $\delta_c = $ const. the deviation of the geometrical axis of the helical coordinates (e.g. $\delta_c = 0$ for LHD). Note that the cylindrical coordinates (R, ϕ, Z) are given as $(R, \phi, Z) = (\sqrt{x^2 + y^2}, -u^3, z)$.

The standard scheme of HINT is shown as follows [1, 2, 3, 4, 5, 6, 7, 8, 9]. The first step (A-step) is a relaxation process of pressure along magnetic field lines under a condition of a fixed magnetic field $\boldsymbol{B}$. To expedite the pressure relaxation, we make an average of pressure, $\bar{p}$, along a field line, and replace a value of pressure at each grid point with the average $\bar{p}$:

$$p(u^1, u^2, u^3) \;\rightarrow\; \bar{p}(u^1, u^2, u^3) = \frac{\int d\ell \; p/|\boldsymbol{B}|}{\int d\ell/|\boldsymbol{B}|}, \tag{6}$$

where ℓ is a length along a field line starting from a grid point (u^1, u^2, u^3). Toroidal periods of tracing a field line are typically 20 - 60 in calculations of this article. In the second step (B-step), calculation of a net toroidal current density $\boldsymbol{j}_{\mathrm{net}}$, e.g. Ohmic current, Ohkawa current and/or bootstrap current, is carried out under conditions of fixed pressure and magnetic field, if a net toroidal current exists in the equilibrium [4, 5, 6, 7]. The third step (C-step) is a relaxation process of magnetic field under a fixed pressure profile:

$$\rho \frac{\partial \boldsymbol{v}}{\partial t} = f_B \Big[-\nabla p + (\boldsymbol{j} - \boldsymbol{j}_0) \times \boldsymbol{B} \Big], \tag{7}$$

$$\frac{\partial \boldsymbol{B}}{\partial t} = -\nabla \times \boldsymbol{E} = \nabla \times \Big\{ \boldsymbol{v} \times \boldsymbol{B} - \eta(\boldsymbol{j} - \boldsymbol{j}_0 - \boldsymbol{j}_{\mathrm{net}}) \Big\}, \tag{8}$$

with a coefficient f_B, which is introduced to relax the Courant-Friedrichs-Levy (CFL) condition [2, 9] on the upper limit of the interval of the computational time step: $\Delta t \leq \Delta u \sqrt{\mu_0 \rho}/(f_B |\boldsymbol{B}|)$, and is defined as

$$f_B = \begin{cases} 1 & \text{for } |\boldsymbol{B}| \leq B_c \\ (B_c/|\boldsymbol{B}|)^2 & \text{for } |\boldsymbol{B}| > B_c, \end{cases} \tag{9}$$

where $\boldsymbol{j} = (1/\mu_0)\nabla \times \boldsymbol{B}$ is the total current density, $\boldsymbol{j}_0 = (1/\mu_0)\nabla \times \boldsymbol{B}_0$ the coil current density: $\boldsymbol{B}_0$ the vacuum magnetic field, and B_c is introduced to smooth the wave propagation with the phase speed of the Alfvén velocity throughout the computation region, which is related to the CFL condition. By introducing the coefficient f_B into the equation of motion, as is shown in equation (7), we are able to easily treat the coil current $\boldsymbol{j}_0$ in the computation region. To calculate an equilibrium with a net toroidal current, we modify the Faraday equation, as is shown in equation (8), which is given by

the following idea [4, 5, 6, 7]. When an equilibrium with a net toroidal current has flux surfaces, Ohm's law can be modified as $\boldsymbol{E}+\boldsymbol{v}\times\boldsymbol{B} = \eta(\boldsymbol{j}-\boldsymbol{B}\langle\boldsymbol{j}\cdot\boldsymbol{B}\rangle_{\rm net}/\langle B^2\rangle)$, where $\langle\cdots\rangle$ means the flux surface average and $\langle\boldsymbol{j}\cdot\boldsymbol{B}\rangle_{\rm net} = \langle\boldsymbol{j}\cdot\boldsymbol{B}\rangle_{\rm ohmic}+\langle\boldsymbol{j}\cdot\boldsymbol{B}\rangle_{\rm bootstrap}+\langle\boldsymbol{j}\cdot\boldsymbol{B}\rangle_{\rm ohkawa}$. Since the existence of nested flux surfaces is not assumed in the HINT code, a toroidal flux is given by using contour lines of pressure. In an island and/or the ergodic region, the flux is estimated by an interpolation. Then the Faraday equation can be extended as

$$\frac{\partial\boldsymbol{B}}{\partial t} = -\nabla\times\boldsymbol{E} = \nabla\times\left\{\boldsymbol{v}\times\boldsymbol{B}-\eta\left(\boldsymbol{j}-\boldsymbol{B}\frac{\langle\boldsymbol{j}\cdot\boldsymbol{B}\rangle_{\rm net}}{\langle B^2\rangle}\right)\right\}. \tag{10}$$

If there exist flux surfaces in a steady state, we have $\langle\boldsymbol{E}\cdot\boldsymbol{B}\rangle = 0 = \eta\left(\langle\boldsymbol{j}\cdot\boldsymbol{B}\rangle - \langle\boldsymbol{j}\cdot\boldsymbol{B}\rangle_{\rm net}\right)$. Thus $\langle\boldsymbol{j}\cdot\boldsymbol{B}\rangle$ becomes $\langle\boldsymbol{j}\cdot\boldsymbol{B}\rangle_{\rm net}$ in a steady state, and we obtain an equilibrium with a net toroidal current. Note that in the HINT computation, a numerical equilibrium on the way to a steady state is not so meaning, and the scheme is justified when the numerical equilibrium relaxes sufficiently into a steady state. In previous studies [4, 5, 6, 7, 9], we verify carefully the validity of equations (7) and (8), and find 'healing' phenomena of magnetic islands, which are caused by effects of a bootstrap current [6] and/or an Ohmic-like toroidal current [7]. In order to express derivatives in space and time, finite differences with fourth-order accuracy are utilized. Solving iteratively the relaxation equations in the above steps, we can find numerically a 3D MHD equilibrium satisfying $\nabla p = (\boldsymbol{j}-\boldsymbol{j}_0)\times\boldsymbol{B}$ with or without a net toroidal current after sufficient iterations.

3. Modified scheme for MHD equilibrium with m/n=1/1 island

In this section, we analyze numerically an LHD equilibrium with an $m/n = 1/1$ island for a finite equilibrium beta $\beta \approx 2$ %. First of all, we set the initial conditions of HINT computation as follows. The vacuum magnetic field is given in a case of $B_{\rm axis} = 4$ T and $R_{\rm axis} = 3.54$ m in a horizontally elongated poloidal cross section, see figure 1, where $B_{\rm axis}$ and $R_{\rm axis}$ are the strength of magnetic field at the magnetic axis and the major radius of the axis, respectively. In this article we consider that the coil currents do not exist in the computation region, i.e. $\boldsymbol{j}_0 = 0$, due to the simplicity of a discussion on a numerical problem shown later. In the standard scheme, of course, the coil currents in the computational region can be treated, but they are one of sources yielding a numerical error in the calculation. The error caused by the coil currents can be easily restrained by making fine meshes, but to avoid the unnecessary error in the discussion on the main subject in this article, we remove the coil currents to out of the computational region. Thus, the vacuum field is given by using filament currents which exist out of the region. We also assume the currentless condition, i.e. the condition of zero net toroidal current, to calculate the equilibrium due to the simplicity. At a horizontally elongated poloidal cross section, Poincaré plots of field lines in the vacuum field with the $m/n = 1/1$ island are given in figure 1(a) and a rotational transform $\iota/2\pi$ is in figure 1(b). As is shown in figure 1, the $m/n = 1/1$ island is formed at the inside of the outermost closed surface

and it provides separation between the flux surfaces and the ergodic field line structure. The O-point of the island is located at $R_{\rm island} = 3.06$ m and $Z_{\rm island} = 0$ m in the poloidal cross section. A width of the island is measured by using the rotational transform $\iota/2\pi \approx 1$, and the width is given as $w_{\rm island} \approx 7.2$ cm along $Z = 0$ in the poloidal cross section. In order to start a relaxation process, we provide an initial pressure profile given as $p = p_{\rm axis}(1 - s)^2$ into the vacuum field, where $p_{\rm axis}$ is a value of pressure at the axis and s the normalized toroidal flux. Note that the pressure profile is not guaranteed to retain its initial shape during the relaxation process; there is no constraint fixing the pressure profile. The profile is changed by the evolution of the relaxation, thus the HINT code can treat naturally formation or healing of islands.

For a case of the equilibrium beta $\beta \approx 2$ %, Poincaré plots of field lines in the LHD equilibrium with the $m/n = 1/1$ island are shown in figure 2(a) and profiles of pressure $p/p_{\rm axis}$ and rotational transform $\iota/2\pi$ are shown in figure 2(b). The O-point of the island is located at $R_{\rm island} = 3.105$ m and $Z_{\rm island} = 0$ m, and the width is given as $w_{\rm island} \approx 12.6$ cm along $Z = 0$ in the poloidal cross section. This equilibrium is calculated by using the standard scheme. In figure 3, we also show Poincaré plots, pressure and rotational transform of the LHD equilibrium *without* the $m/n = 1/1$ island, where difference between them is existence of an error magnetic field causing the $m/n = 1/1$ island in vacuum. From comparisons between them, they are similar each other, except in and around the island; both magnetic axes are located at $R_{\rm axis} = 3.74$ m and $Z_{\rm axis} = 0$ m in the poloidal cross section, and profiles of pressure and rotational transform as functions of toroidal flux are similar each other, as is shown in figure 4. In the HINT computation, the existence of nested flux surfaces is not assumed. The toroidal flux is calculated by using contour lines of pressure, and it can be given in the island and the ergodic region by using an interpolation. Note that a pressure in the ergodic region is rarefied but remains because of long connection length of a field line from the region to the wall, as is shown in figures 2 and 3. The numerical analysis of the equilibrium with the island seems to succeed outwardly, however, error of force balance $\langle E_f \rangle$ plotted as solid triangles in figure 5 is large, thus the equilibrium in figure 2 is not numerically appropriate as compared with the case without the island plotted as solid squares, where $\langle E_f \rangle$ is defined as

$$\langle E_f \rangle = \frac{\int dV |\nabla p - (\boldsymbol{j} - \boldsymbol{j}_0) \times \boldsymbol{B}|^2}{\int dV (|\nabla p|^2 + |(\boldsymbol{j} - \boldsymbol{j}_0) \times \boldsymbol{B}|^2)}. \tag{11}$$

Reduction of the error for the case with the island is very slow, and it seems to be difficult to have an appropriate numerical equilibrium. Unfortunately, though the mesh size and/or the toroidal periods of tracing a field line in the A-step are set better, the error is not effectively reduced. To fix a source of the large error, we should investigate a profile of the error, $E_f(u_1, u_2, u_3)$, in detail, where $E_f(u_1, u_2, u_3) = |\nabla p - (\boldsymbol{j} - \boldsymbol{j}_0) \times \boldsymbol{B}|^2 / \int dV (|\nabla p|^2 + |(\boldsymbol{j} - \boldsymbol{j}_0) \times \boldsymbol{B}|^2)$. The profile of the error $E_f(u_1, u_2, u_3)$ at, for example, the vertically elongated poloidal cross section ($u_3 = 0$ at the cross section) given in figure 6(a) is shown in figure 7(a). These figures are given at the step pointed by arrow (a) in figure 5. We find that the error concentrates extremely

on the separatrix of the island, and on the other hand the error in the core region within $\iota/2\pi = 1$ is negligibly small. The error in the core region seems to be sufficiently reduced, as is also estimated as an asterisk in figure 5. This fact is consistent with the similarity between both results in the cases with and without the island. As a result, the numerical equilibrium with the island shown in figure 2 may be enough to sufficiently relax except in and around the island; but our aim to have the appropriate numerical equilibrium with the island is not accomplished. It is necessary to reduce the error around the island, in order to measure appropriately the magnetic field line structure and profiles of $p/p_{\rm axis}$ and $\iota/2\pi$ in and around the island. As is shown in figure 8(a), the source of error of force balance is fixed on an error of ∇p-calculation. Since the relaxation process of pressure in the standard scheme is expressed as only the parallel diffusion of pressure, propagation of information on the pressure across a field line is neglected; i.e. values of pressure between even the nearest-neighbor closed surfaces are determined independently each other. In the island, the pressure becomes almost flat and its value is changed steeply as compared with neighbor closed surfaces, thus the pressure profile becomes discontinuous at the separatrix of the island and a derivative of the pressure at the separatrix is not well-behaved. Actually, the error of ∇p is located on the separatrix of the island, as is shown in figure 8(a). Mathematically indeed there is a possibility that a delta-function of current, i.e. $\delta \boldsymbol{j} \times \boldsymbol{B}$, is balanced with ∇p at the discontinuity of pressure, but the delta-function-like current balancing sufficiently with the delta-function-like ∇p is not observed; though the mesh size is set better, the error is not so improved. We guess that it is difficult to generate such a current, because 1) Fourier components of magnetic fields caused by the $m/n = 1/1$ island are weak and entirely alien from ones in the original equilibrium (i.e. the LHD equilibrium with the stellarator symmetry), 2) the island has a large width (e.g. a change of pressures at the separatrix of the island becomes large, the discontinuity of pressure is not so affected by the relaxation process of magnetic field, etc.), 3) it exists at the edge region, and 4) it is surrounded by the ergodic region, as is shown in figure 2(a). In general, if there is an island in an equilibrium given by using the standard scheme, the force balance $|\nabla p - (\boldsymbol{j} - \boldsymbol{j}_0) \times \boldsymbol{B}|$ around the island is deteriorated as compared with in an equilibrium without the island. However, when islands yield Fourier components of magnetic fields with the toroidal period of helical coils, this problem is not so serious, as is shown by a dash line in figure 5. The difficulty is remarkable when the island yields different Fourier components of magnetic fields from ones with the toroidal period. It is not so clear why the error for the case with the toroidal period is negligibly small; the reason is guessed above, and it will be studied in detail in near future.

Unfortunately, there is no process to resolve the problem in the standard scheme of the HINT computation, because the relaxation process of pressure is assumed to proceed along field lines. In order to reduce the error of ∇p, the relaxation process across the field lines is needed. To modify the standard scheme, we return to the original MHD

equations [18]. In the MHD equations, the evolution of pressure is described as

$$\frac{\partial p}{\partial t} = -\boldsymbol{v}\cdot\nabla p - \gamma p\nabla\cdot\boldsymbol{v} + \rho\nabla\cdot\left[\overleftrightarrow{\kappa}\cdot\nabla\left(\frac{p}{\rho}\right)\right]. \tag{12}$$

The relaxation process of pressure in the standard scheme is derived as follows [1, 2, 3, 18]. The parallel sound wave and the large parallel thermal conductivity $\kappa_{\|}$ ($\kappa_{\|} \gg \kappa_{\perp}$) in equation (12) give a constant pressure along a field line, $\boldsymbol{B}\cdot\nabla p = 0$. Since the pressure relaxation described in equation (12) is excepted to be so slow, we adopt an artificial method expressing the parallel relaxation process in equation (6) to accelerate the process. However, when a gradient of the pressure is not well-behaved, it is natural to consider the perpendicular diffusion of pressure, because the perpendicular diffusion is included originally in the MHD equations and the problem is caused by neglecting this process. To avoid handling highly time-consuming scheme of equation (12), we need to solve independently an artificial diffusion process due to the acceleration of the pressure relaxation. Thus, in order to reduce an error of force balance around the island, we consider an artificial diffusion process of the error $E_f \sim \nabla p - (\boldsymbol{j}-\boldsymbol{j}_0)\times\boldsymbol{B} = \nabla(p-p_*)$ as follows:

$$\frac{\partial(p-p_*)}{\partial t} = \kappa\nabla^2(p-p_*) = \kappa\nabla\cdot\Big(\nabla p - (\boldsymbol{j}-\boldsymbol{j}_0)\times\boldsymbol{B}\Big), \tag{13}$$

where κ is a small diffusion constant and $\nabla p_* = (\boldsymbol{j}-\boldsymbol{j}_0)\times\boldsymbol{B}$ is not a function of time, i.e. $\partial p_*/\partial t = 0$, because $\boldsymbol{B}$ is fixed in the A-step. Therefore, a modified scheme of the A-step consists of the following relaxation processes; first, the pressure relaxation for the parallel direction is evolved by tracing field lines

$$p(u^1,u^2,u^3) \;\rightarrow\; \bar{p}(u^1,u^2,u^3) = \frac{\int d\ell\; p/|\boldsymbol{B}|}{\int d\ell/|\boldsymbol{B}|}, \tag{14}$$

and after the parallel process, the diffusion of the error is done:

$$\frac{\partial p}{\partial t} = \kappa\nabla\cdot\Big(\nabla p - (\boldsymbol{j}-\boldsymbol{j}_0)\times\boldsymbol{B}\Big). \tag{15}$$

By using the modified scheme of pressure relaxation which starts from the numerical equilibrium data just before the step pointed by arrow (b) in figure 5, the error of force balance is improved clearly, as is plotted as solid circles in figure 5. Both errors of $E_f(u_1,u_2,u_3)$ and ∇p are reduced, which are shown in figures 7(b) and 8(b) at the vertically elongated poloidal cross section ($u^3 = 0$) in figure 6(b). These figures are given by using the modified scheme at the step pointed by arrow (a) in figure 5. After sufficient time when the relaxation is enough to numerically satisfy $\nabla p = (\boldsymbol{j}-\boldsymbol{j}_0)\times\boldsymbol{B}$, we have that $\boldsymbol{B}\cdot\nabla p$ becomes negligibly small; the error of $\boldsymbol{B}\cdot\nabla p$ is computed as $\int dV|\boldsymbol{B}\cdot\nabla p|/\int dV|\boldsymbol{B}|\,|\nabla p| < 10^{-7}$ in calculations using the modified scheme. Poincaré plots of field lines and profiles of $p/p_{\rm axis}$ and $\iota/2\pi$ are given in figure 9 for the case of the modified scheme. We see that both results in the standard and modified schemes are similar each other. For the modified scheme, the magnetic axis is located at $R_{\rm axis} = 3.73$ m and $Z_{\rm axis} = 0$ m in the poloidal cross section, and profiles of pressure and rotational transform are similar to results given by the standard scheme, as is shown in figure 4.

Since the central beta value decreases slightly due to the diffusion process, the Shafranov-shift of the axis is a little bit small as compared with one in the standard scheme. Note that absolute values of pressure around the axis decrease slightly because the pressure diffuses to around the island, but the shape of the pressure profile is not almost changed, as is shown in figure 4. The O-point of the island is located at $R_{\rm island} = 3.104$ m and $Z_{\rm island} = 0$ m, and the width is measured as $w_{\rm island} \approx 13.3$ cm along $Z = 0$ in the poloidal cross section. On the other hand, in and around the island the profile of pressure given by the modified scheme differs from results of the standard one; it is caused by the diffusion process of equation (15). Ergodic field line structure around the island, which has a long connection length, is changed to be somewhat wide. We guess that it is caused by the diffusion process of equation (15) and reduction of the numerical error around the island. The mesh dependence of results in the modified scheme is given by comparison between the case with meshes $N_{u_1} \times N_{u_2} \times N_{u_3} = 97 \times 97 \times 324$ (solid circle) and the case with $49 \times 49 \times 324$ (open circle) in figure 5. We see that the error of force balance is improving with reducing the mesh size. Unfortunately, an equilibrium calculation with more fine meshes is not carried out because of the computer's performance, however, the validity of modified scheme is justified.

In the vacuum field, since the $m/n = 1/1$ island is located within the outermost closed surface, almost all particles are expected to drift into the island, see figure 1. On the other hand, as is shown in figure 9, the island in the equilibrium with $\beta \approx 2$ % is surrounded with ergodic field lines, and a performance of the island divertor may be deteriorated because a part of particles can escape to the wall, which are guided along field lines in the ergodic region.

4. Conclusions

From the HINT computations under the currentless condition for $\beta \approx 2$ %, we see the following results. 1) By using the standard scheme, the LHD equilibrium with the $m/n = 1/1$ island can be calculated, but it is not numerically appropriate in and around the island. Thus, when we need to have accurate equilibrium data in and around the island, the standard scheme is not suited. Note that the problem is remarkable when the island yields different Fourier components of magnetic fields from ones with the toroidal period of helical coils. Difference of the error for islands with and without the toroidal period will be studied in near future. In the standard scheme, a derivative of the pressure at the separatrix of the island is not well-behaved, and the perpendicular diffusion of pressure should be considered to resolve the problem. We modify the scheme, and solve the diffusion process of the error of force balance instead of solving directly the perpendicular diffusion of pressure. The modified scheme reduces clearly the error of force balance, and the validity of modified one is justified by comparing results calculated in the different meshes. Note that the scheme is justified when the numerical equilibrium relaxes sufficiently into a steady state with negligibly small error of force balance. The scheme solving the diffusion process of the error of force balance has several advantages.

(a) Effects of the diffusion process should be reduced with evolving the relaxation process. If the numerical equilibrium satisfies the condition of the sufficiently small error of force balance, the r.h.s. of the equation of the diffusion described in equation (15) is negligible. And results given by the modified scheme does not depend on a value of the diffusion constant κ; the constant κ is required only to be a sufficiently small number. (b) It does not disturb a region already satisfying the condition of the sufficiently small error in the equilibrium data given by the standard scheme, as is shown in figure 4. This advantage is very convenient to start from the equilibrium data given by the standard scheme, and to compare both results in the standard and the modified one. 2) In the LHD equilibrium with the $m/n = 1/1$ island, good flux surfaces with the island are preserved, but the island divertor with the $m/n = 1/1$ island may be deteriorated because of the existence of the ergodic region between the closed surfaces and the island. These results are sensitive to an initial pressure profile and a net toroidal current, thus investigations of dependence on pressure and net toroidal current are required. And a transport analysis of particles drifting into the island is needed to evaluate a performance of the island divertor. They are going to be studied and will be reported in near future.

Acknowledgements

One of the authors (Kanno) thanks Dr. R. Ishizaki for his useful suggestions. This work was supported by a Grant-in-Aid from the Ministry of Education, Culture, Sports, Science and Technology, No. 12780369.

References

[1] Hayashi T 1989 *Theory of Fusion Plasmas* (Varenna) 11
[2] Harafuji K, Hayashi T and Sato T 1989 *J. Comput. Phys.* **81** 169
[3] Hayashi T, Sato T, Markel P, Nührenberg J and Schwenn U 1994 *Phys. Plasmas* **1** 3262
[4] Kanno R, Nakajima N, Hayashi T and Okamoto M 1998 *J. Plasma Fusion Res. SERIES* **1** 488
[5] Kanno R, Nakajima N, Hayashi T and Okamoto M 1999 *J. Plasma Phys.* **61** 213
[6] Kanno R, Nakajima N, Hayashi T, Yokoyama M and Okamoto M 1999 *J. Plasma Fusion Res. SERIES* **2** 291
[7] Kanno R, Nakajima N, Hayashi T and Okamoto M 2000 *J. Plasma Fusion Res. SERIES* **3** 584
[8] Kanno R, Nakajima N, Hayashi T and Okamoto M 2000 *Contrib. Plasma Phys.* **40** 260
[9] Hayashi T, Miura H, Kanno R, Nakajima N, Okamoto M and Sato T 2002 *Contrib. Plasma Phys.* **42** 309
[10] Komori A *et al* 1995 *Plasma Physics and Controlled Nuclear Fusion Research* (Vienna) **II** 773
[11] Ohyabu N *et al* 1995 *J. Nucl. Mater.* **220-222** 298
[12] Morisaki T *et al* 2000 *J. Plasma Fusion Res. SERIES* **3** 188
[13] Morisaki T *et al* 2002 *Contrib. Plasma Phys.* **42** 321
[14] Morris R N 1989 *Nucl. Fusion* **29** 2115
[15] Gardner H J 1990 *Nucl. Fusion* **30** 1417
[16] Morisaki T *et al* 2000 *Contrib. Plasma Phys.* **40** 266
[17] Hirshman S P, van Rij W I and Merkel P 1986 *Comput. Phys. Commun.* **43** 143
[18] Park W, Monticello D A, Strauss H and Manickam J 1986 *Phys. Fluids* **29** 1171

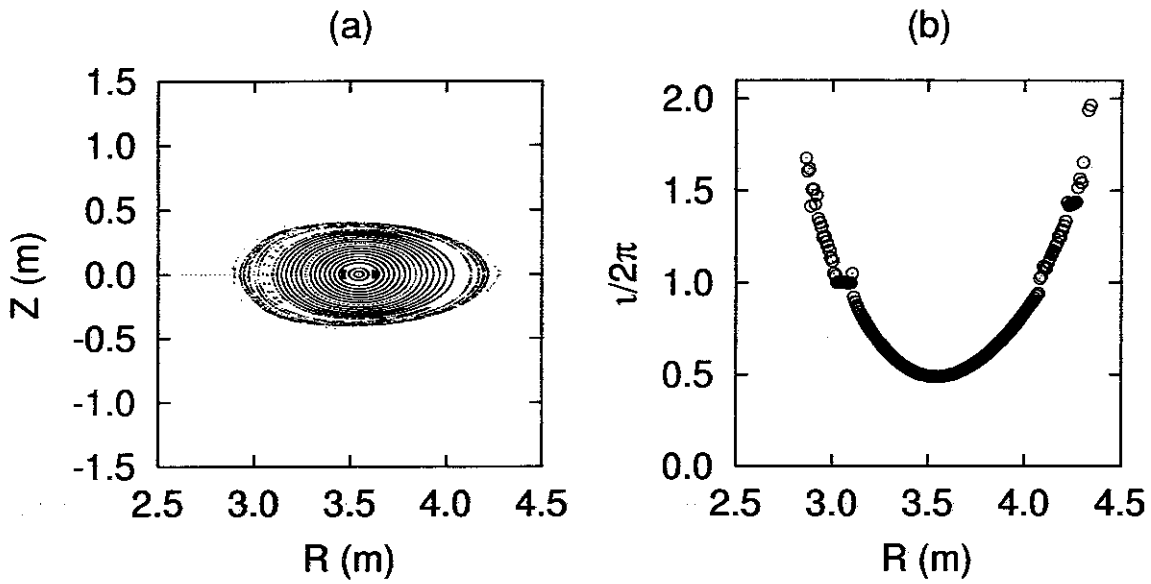

Figure 1. (a) Poincaré plots of field lines at the horizontally elongated poloidal cross section and (b) profiles of rotational transform $\iota/2\pi$ (open circle) along $Z = 0$ in the horizontally elongated poloidal cross section in the vacuum field configuration with the $m/n = 1/1$ island. Plots of $\iota/2\pi$ are set at equal intervals along $Z = 0$, and a value of $\iota/2\pi$ is calculated by tracing a field line. Magnetic axis is located at $R_{\rm axis} = 3.54$ m and $Z_{\rm axis} = 0$ m. The O-point of the island is located at $R_{\rm island} = 3.06$ m and $Z_{\rm island} = 0$ m, and the width of the island is measured as $w_{\rm island} \approx 7.2$ cm along $Z = 0$.

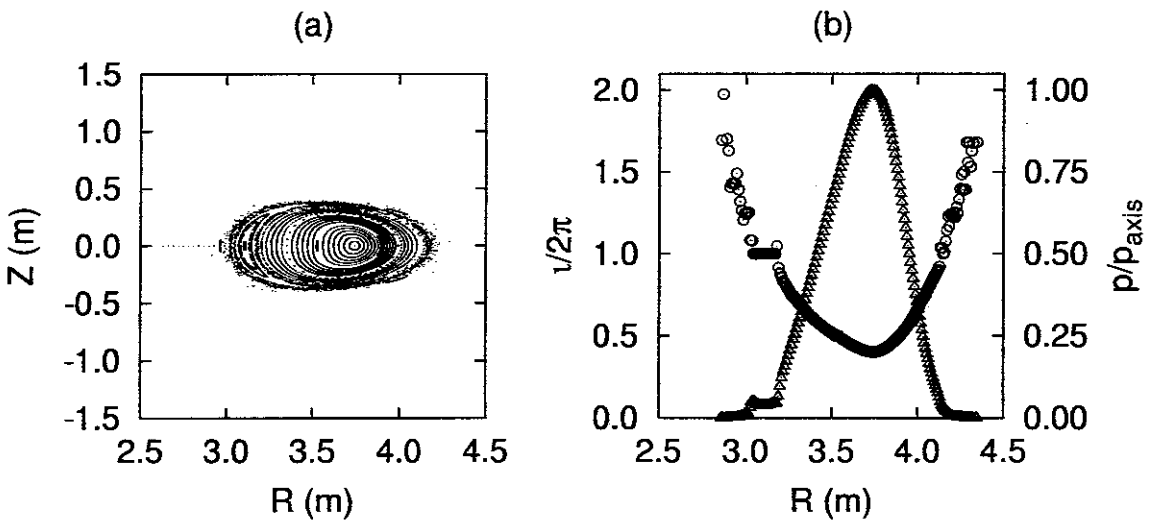

Figure 2. (a) Poincaré plots of field lines and (b) profiles of rotational transform $\iota/2\pi$ (open circle) and pressure $p/p_{\rm axis}$ (open triangle) along $Z = 0$ in the LHD equilibrium with the $m/n = 1/1$ island for $\beta \approx 2$ %. Values of pressure between grid points are calculated by an interpolation. These figures are given by using the standard scheme with meshes $N_{u_1} \times N_{u_2} \times N_{u_3} = 97 \times 97 \times 324$ at the step pointed by arrow (a) in figure 5, where N_{u_1}, N_{u_2} and N_{u_3} are number of meshes for the u_1, u_2 and u_3 directions, respectively. Magnetic axis is located at $R_{\rm axis} = 3.74$ m and $Z_{\rm axis} = 0$ m. The O-point of the island is located at $R_{\rm island} = 3.105$ m and $Z_{\rm island} = 0$ m, and the width of the island is measured as $w_{\rm island} \approx 12.6$ cm along $Z = 0$.

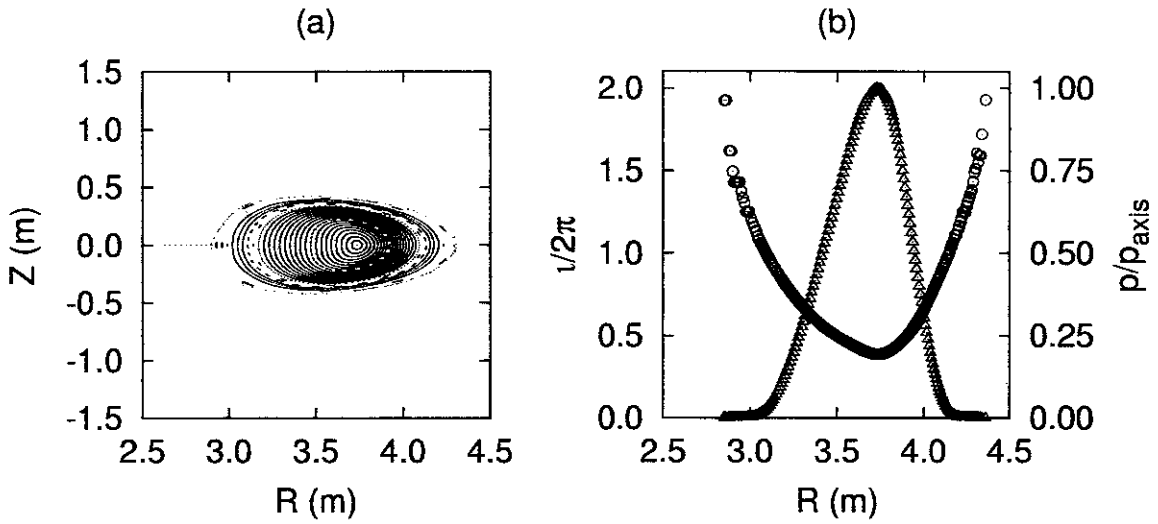

Figure 3. (a) Poincaré plots of field lines and (b) profiles of rotational transform $\iota/2\pi$ (open circle) and pressure $p/p_{\rm axis}$ (open triangle) along $Z = 0$ in the LHD equilibrium without the $m/n = 1/1$ island for $\beta \approx 2$ %. These figures are given by using the standard scheme with meshes $97 \times 97 \times 324$ at the step pointed by arrow (a) in figure 5. Magnetic axis is located at $R_{\rm axis} = 3.74$ m and $Z_{\rm axis} = 0$ m.

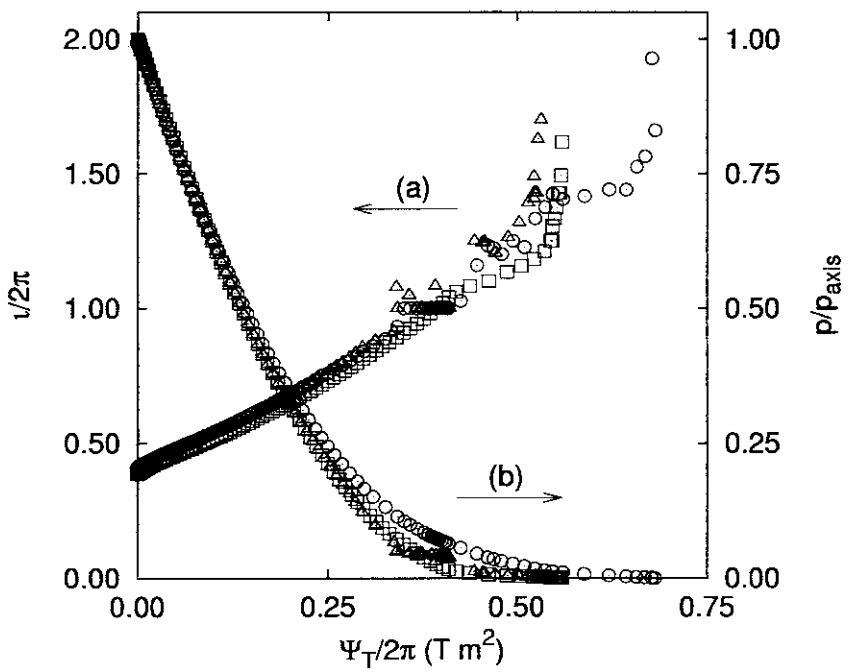

Figure 4. Profiles of (a) rotational transform $\iota/2\pi$ and (b) pressure $p/p_{\rm axis}$ as functions of toroidal flux $\Psi_{\rm T}/2\pi$ T m^2 in the LHD equilibrium for $\beta \approx 2$ %. Each plot has the meaning as follows; (1) open triangle: profile given by the standard scheme for the equilibrium with the $m/n = 1/1$ island, (2) open square: profile given by the standard scheme for the equilibrium without the island, and (3) open circle: profile given by the modified scheme for the equilibrium with the island. These figures are given by using the equilibrium data with meshes $97 \times 97 \times 324$ at the step pointed by arrow (a) in figure 5.

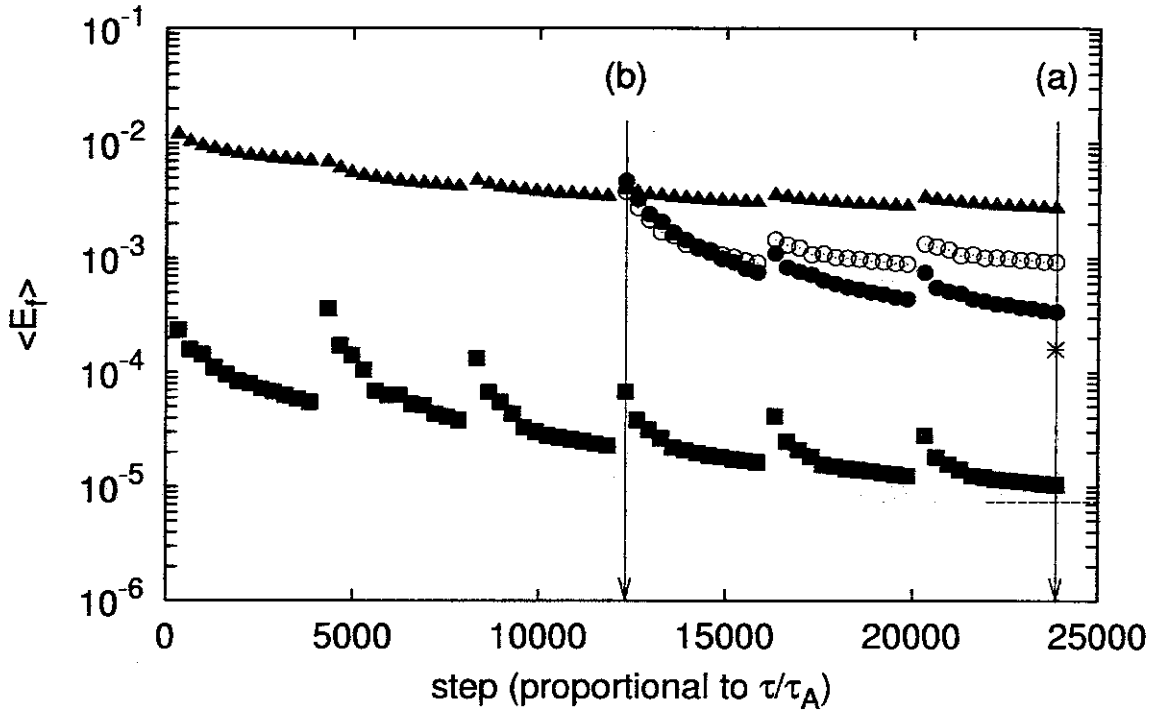

Figure 5. Error of force balance $\langle E_f \rangle$ as a function of number of iterations (step) for the LHD equilibrium with $\beta \approx 2$ %, where number of iterations is proportional to τ/τ_A, τ is time in the simulations and τ_A is the Alfvén time. The errors just after starting up the calculations are cut out from this figure. Computations for the equilibrium with the $m/n = 1/1$ island are carried out in the several cases plotted by (1) solid triangle, (1') asterisk, (3) solid circle and (4) open circle; and computations for the equilibrium without the $m/n = 1/1$ island are done in the case plotted by (2) solid square. Each plot has the meaning as follows; (1) solid triangle: error of the standard scheme with meshes $N_{u_1} \times N_{u_2} \times N_{u_3} = 97 \times 97 \times 324$, (1') asterisk: error of the standard scheme with meshes $97 \times 97 \times 324$, which is estimated inward the error around the island shown in figure 7(a), (2) solid square: error of the standard scheme with meshes $97 \times 97 \times 324$, (3) solid circle: error of the modified scheme with meshes $97 \times 97 \times 324$, and (4) open circle: error of the modified scheme with meshes $49 \times 49 \times 324$. A dash line means a level of the error estimated in a previous study with the standard scheme of the HINT code [3], where islands generating in an equilibrium of the previous study yield Fourier components of magnetic fields with the toroidal period of helical coils (or external coils except island control coils) and the error is calculated by using meshes $73 \times 73 \times 41$ for a half-pitch of a toroidal period of an equilibrium with a stellarator symmetry ($73 \times 73 \times 364$ for converting into a period of full torus). We give several figures of the equilibrium at the step pointed by arrow (a) in this article. The modified scheme of pressure relaxation starts from the numerical equilibrium data given by the standard scheme just before the step pointed by arrow (b).

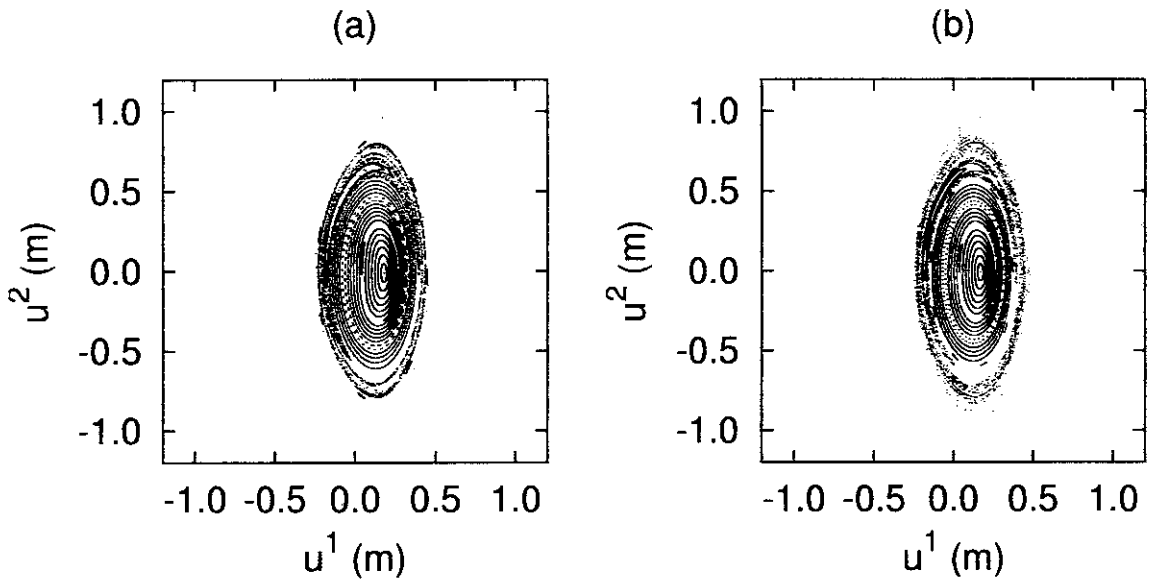

Figure 6. Poincaré plots of field lines at the vertically elongated poloidal cross section ($u_3 = 0$) in the LHD equilibrium with the $m/n = 1/1$ island for $\beta \approx 2$ %, given by (a) the standard scheme and (b) the modified scheme, at the step pointed by arrow (a) in figure 5. These figures are given by using the equilibrium data with meshes $97 \times 97 \times 324$. Magnetic axes are located at (a) $R_{\rm axis} = 3.78$ m and $Z_{\rm axis} = 0$ m, and (b) $R_{\rm axis} = 3.77$ m and $Z_{\rm axis} = 0$ m.

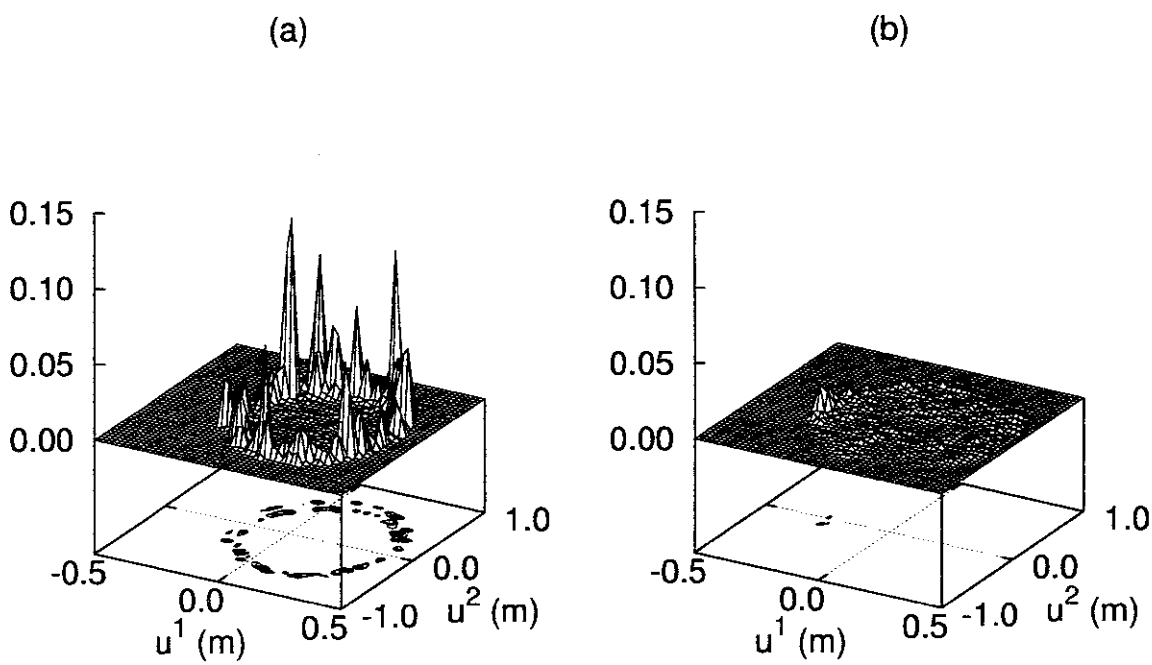

Figure 7. Strength of error $E_f(u_1, u_2, u_3)$ (a.u.) at the vertically elongated poloidal cross section ($u_3 = 0$) in the LHD equilibrium with the $m/n = 1/1$ island for $\beta \approx 2$ %, given by (a) the standard scheme and (b) the modified scheme, at the step pointed by arrow (a) in figure 5. In figure (a), the error concentrates extremely on the separatrix of the island. On the other hand, in figure (b) the error is reduced almost uniformly. These figures are calculated by using the equilibrium data with meshes $97 \times 97 \times 324$.

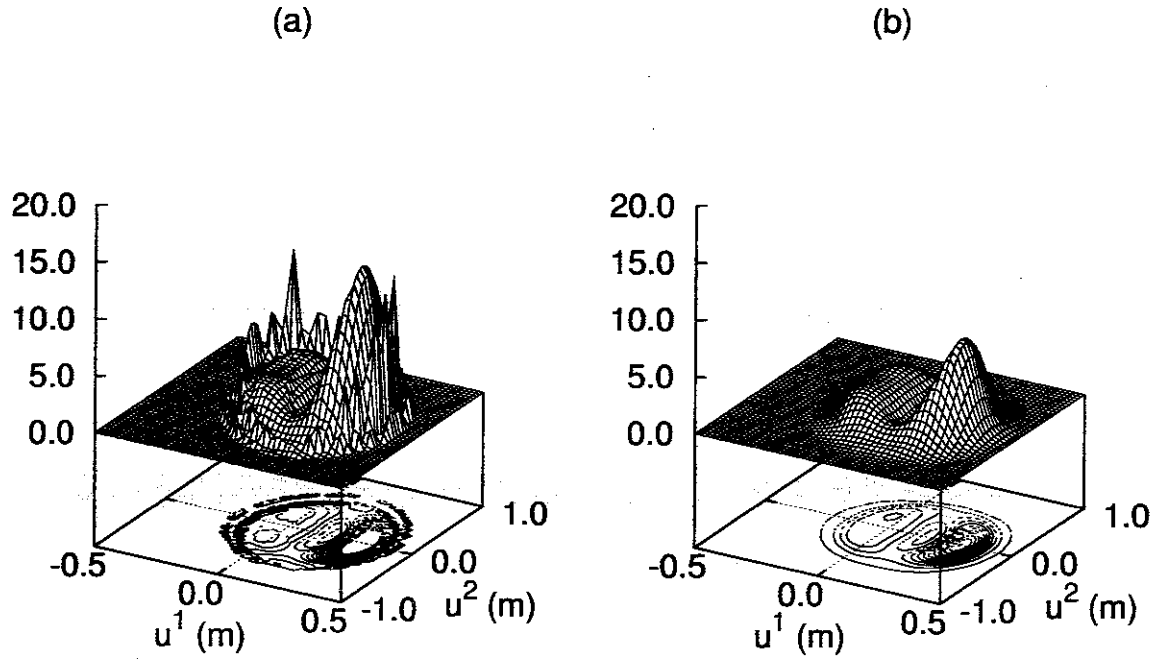

Figure 8. Strength of $|\nabla p(u_1, u_2, u_3)|^2$ (a.u.) at the vertically elongated poloidal cross section ($u_3 = 0$) in the LHD equilibrium with the $m/n = 1/1$ island for $\beta \approx 2$ %, given by (a) the standard scheme and (b) the modified scheme, at the step pointed by arrow (a) in figure 5. In figure (a), the error of ∇p is located on the separatrix of the island. On the other hand, in figure (b) the error is negligible. These figures are calculated by using the equilibrium data with meshes $97 \times 97 \times 324$.

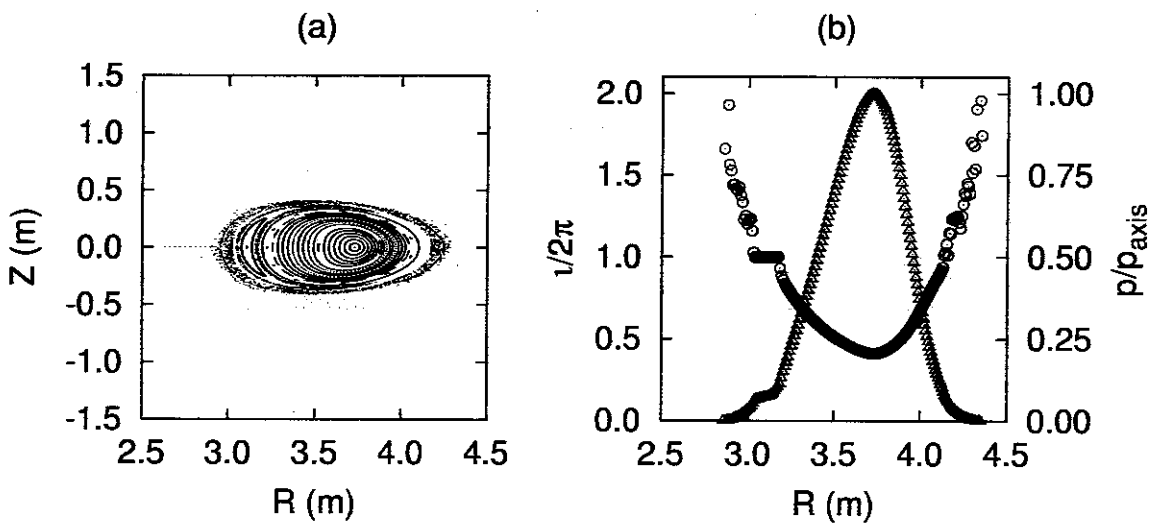

Figure 9. (a) Poincaré plots of field lines and (b) profiles of rotational transform $\iota/2\pi$ (open circle) and pressure $p/p_{\rm axis}$ (open triangle) along $Z = 0$ in the LHD equilibrium with the $m/n = 1/1$ island for $\beta \approx 2$ %. These figures are given by using the modified scheme with meshes $97 \times 97 \times 324$ at the step pointed by arrow (a) in figure 5. We switch the scheme of pressure relaxation from the standard to the modified one at the step pointed by arrow (b) in figure 5. Magnetic axis is located at $R_{\rm axis} = 3.73$ m and $Z_{\rm axis} = 0$ m. The O-point of the island is located at $R_{\rm island} = 3.104$ m and $Z_{\rm island} = 0$ m, and the width of the island is measured as $w_{\rm island} \approx 13.3$ cm along $Z = 0$.